OPEN ACCESS
IOP Publishing | The Japan Society of Fluid Mechanics Fluid Dynamics Research
Fluid Dyn. Res. **55** (2023) 015501 (22pp) https://doi.org/10.1088/1873-7005/acafa1

Rheology, rheometers, and matching models to experiments

L Ridgway Scott

University of Chicago, Chicago, IL, United States of America

E-mail: ridg@uchicago.edu

Received 7 October 2022; revised 19 December 2022
Accepted for publication 3 January 2023
Published 19 January 2023

Communicated by Professor Hyung Jin Sung

Abstract

We consider the general problem of matching rheological models to experiments. We introduce the concept of *identifiability* of models from a given set of experiments. To illustrate this in detail, we study two rheology models, the grade-two and Oldroyd 3-parameter models, and consider two hypothetical rheometers to see if the coefficients of the rheology models are identifiable from experimental measurements or not. For the Oldroyd models, we show that the coefficients can be estimated from experiments from the two rheometers. But for the grade-two model, it is not possible to distinguish the two nonNewtonian parameters, only their sum can be estimated, and thus the grade-two model is not identifiable by the two hypothetical rheometers. However, our results imply that a different rheometer may be able to do that.

Keywords: rheology, rheometers, identifiability

There are many models for non-Newtonian fluids, as highlighted by the so-called Rheology Drugstore of Joseph (2013). Similarly, there are many types of rheometers (Lodge *et al* 1991, Gallot *et al* 2013, Nyström *et al* 2017) designed to measure the properties of different fluids. Our goal here is to consider a small subset of each and ask the question: to what extent do the rheometers distinguish coefficients in different models?

The next objective is to turn this question around, and ask what coefficients in different models best match experimental data, and ultimately, which model bests fits the experiments (Robert *et al* 1985). However, the prerequisite for such a study is the requirement that given rheometers can distinguish the different parameters, a property that we can describe as *identifiability*.

To begin this study, we consider two different rheology models: the grade-two model (Girault and Scott 2001) and the Oldroyd models (Girault and Scott 2018). We chose these models in part because of the Tanner (1982), Girault and Scott (2021a, 2021b)duality property for these models. There are of course many other models that are used for rheology.

1873-7005/23/015501+22$33.00

One simple but popular one is the power-law model. This has been extensively studied (Saramito 2016).

We begin by considering geometries and flow profiles that provide exact solutions for these models, for two reasons. First of all, they give test problems for computer simulation codes. But more importantly, they allow a clear view of what a given rheometer will distinguish in a given model, or not. More realistic rheometer designs are considered in Pollock and Scott (2022b).

We describe two hypothetical rheometers related to the exact solutions for the two models, both of which involve two parameters in addition to viscosity. We will show that the Oldroyd model is identifiable with these two rheometers but the grade-two model is not. On the other hand, recent computational evidence (Pollock and Scott 2022b) indicates that the grade-two model is identifiable by a contraction rheometer (Nyström *et al* 2017).

The state of rheology model theory has advanced recently with the advent of rigorous mathematical analyses of some models (Cioranescu *et al* 2016). This includes both the establishment of a foundational theory for the system of partial differential equations and associated boundary conditions, as well as numerical methods for solving the equations. Despite recent advances in these directions (Pollock and Scott 2022a, 2022c), much still needs to be done to clarify important properties of popular models. A review of Bird *et al* (1987) indicates the breadth of models that would need to be considered.

We limit our purview to steady flows. Determining rheological properties from time-dependent flows is likely much more complicated.

1. Rheology modeling challenge

The challenge of rheology modeling is to match apples and oranges. Let us say that the apples are the models, of which there are many (Joseph 2013), and they have many parameters. The oranges are rheological measurements, done by devices called rheometers, essentially machines that do experiments to determine quantities such as a force as a function of flow rate.

Experimental quantities and concepts include

- normal-stress difference (Lodge *et al* 1991),
- excess pressure drop (Nyström *et al* 2017)
- extensional viscosity (Petrie 2006),
- apparent viscosity (Tanveer *et al* 2006),
- shear thinning/thickening (dilatant),
- rheopectic versus thixotropic (time dependent).

How do we match them to models? A quote by Pearson in Petrie (2006) sums up the challenge this way:

> '… if you want to predict flow in all circumstances, you need a REoS [a rheological equation of state or constitutive equation], nothing less. Rheometric functions can be useful in classification and categorization, involving qualitative statements, and can provide engineering approximations in particular flow fields, but they cannot be inserted in CFD packages.'

In a very simple case, we can consider a particular model (e.g. Oldroyd) and ask how we can determine its parameters $\mathbf{x}$ from the measurements $\mathbf{y}$ of a given rheometer, or multiple rheometers. What computational simulations of rheometers produce is $\mathbf{y} = f(\mathbf{x})$. But we want

to determine an inverse function $\mathbf{x} = g(\mathbf{y})$. To do so, we need to know if the given rheometer can distinguish the parameters $\mathbf{x}$ of the model. That is, for different values of $\mathbf{x}$, do you get some different data $\mathbf{y}$? If not, then there could be multiple $\mathbf{x}$ for a single $\mathbf{y}$, and so g is not a function. We will see that, for example, measurements from a shear-flow rheometer will be identical, independent of the key parameter of the grade-two model. Thus it may not be possible to find a function g just using that one rheometer.

The parameters of a model cannot be reliably determined from a single experiment, or even a number of experiments matching the number of parameters. Rather, a larger set of experiments are used to determine parameters. For example, this can be done by varying the flow rate, and thus the Reynolds number, e.g. by simply increasing the flow rate as a function of time and measuring the resulting experimentally determined data. The flow rate can be stabilized at different times to insure steady flow is established at each successive Reynolds number.

2. Rheology models

All models of steady flow have the basic equation

$$\mathbf{u}\cdot\nabla\mathbf{u} + \nabla p = \nabla\cdot\mathbf{T}, \tag{2.1}$$

where $\mathbf{T}$ is the extra (or deviatoric) stress. The models only differ depending on how the stress is related to the velocity $\mathbf{u}$. In the case of a Newtonian fluid

$$\mathbf{T} = \nu\mathbf{A}\,,$$

where ν is the kinematic viscosity (Landau and Lifshitz 1959) and $\mathbf{A} = \nabla\mathbf{u} + (\nabla\mathbf{u})^t$. Thus, when $\nabla\cdot\mathbf{u} = 0$, it follows that $\nabla\cdot\mathbf{T} = \nu\Delta\mathbf{u}$, and we obtain the well known Navier–Stokes equations for Newtonian flow,

$$-\nu\Delta\mathbf{u} + \mathbf{u}\cdot\nabla\mathbf{u} + \nabla p = \mathbf{f} \tag{2.2}$$

where $\mathbf{f}$ is a possible body force. Table 1 gives the kinematic viscosity ν for various fluids at various temperatures. One feature indicated by the table is that gases increase in viscosity as temperature is increased, whereas liquids decrease in viscosity as temperature is increased. The unit chosen (stokes) makes it natural to measure lengths in centimeters and fluid speeds in centimeters per second. For many rheometers, these are natural units.

Typically, nonhomogeneous boundary conditions are imposed: $\mathbf{u} = \mathbf{g}$ on $\partial\Omega$, the bounding surface of the volume Ω.

2.1. Viscosity definition

The dynamic (or absolute) viscosity μ is defined typically as the ratio of stress σ and strain rate:

$$\mu\frac{\partial v}{\partial x} = \sigma. \tag{2.3}$$

Stress is defined as the force per unit area across an infinitesimal surface. Force has units ML/T^2, so stress has units $M/(LT^2)$. Therefore the units in (2.3) are consistent. But v and x are vector quantities, so in general μ would have to be a tensor of order (or arity) 4 in general (Nunan and Keller 1984). For Newtonian fluids, this tensor reduces to a scalar times the identity tensor.

Table 1. Kinematic viscosity coefficients in stokes ($cm^2\ s^{-1}$) for various fluids (Kestin *et al* 1978, Gokdogan *et al* 2015).

Fluid	Kinematic viscosity	Conditions
Castor oil	2.41	T =40 $C = 104$ F
Air	0.100	$T = -40$ $C = -40$ F
Air	0.170	$T = 40$ $C = 104$ F
Water	0.010	$T = 20$ $C = 68$ F
Water	0.006	$T = 45$ $C = 113$ F
Mercury	0.001	$T = 20$ $C = 68$ F

The units of μ are mass divided by length$\times$time, and the units of mass density ρ are mass divided by length cubed. Thus the units of μ/ρ are

$$\frac{M/(LT)}{M/L^3} = \frac{L^2}{T}$$

which are the units for diffusion.

The kinematic viscosity ν is simply μ/ρ. Table 1 gives the kinematic viscosity for various fluids under various conditions.

2.2. Apparent viscosity

Apparent viscosity is typically defined as (2.3) without significant elaboration. In Nijenhuis *et al* (2007), more complicated notions are explored. But there are various ways to generate $\mathbf{v}$ and the resulting $\boldsymbol{\sigma}$ will often have several components. So a precise experimental or computational framework is necessary to make a clear definition. Here we will give two such examples. We will see that the ultimate relationship is tensorial, so it is not so clear how to define a scalar value for 'viscosity.' Indeed, we seem to be lacking a good term to explain the principal effect of rheology beyond Newtonian viscosity. One way is simply to define the apparent viscosity ν_a as

$$\nu_a(\mathbf{v}) = \frac{\|\mathbf{T}\|}{\|\nabla\mathbf{v}\|} \tag{2.4}$$

for some norm on matrices, where $\mathbf{T}$ is the observed stress related to the flow velocity $\mathbf{v}$. The same fluid could produce different values of apparent viscosity in different flow geometries, however.

2.3. Thin/thick-ening

If we use the definition (2.4) for apparent viscosity, then we can say that the fluid is thinning if

$$\nu_a(t\mathbf{v}) < \nu_a(\mathbf{v})$$

when $t > 1$. When this holds for the expression (2.4) involving a norm, then any other notion thinning would also apply. But (2.4) may be too strong to catch subtle behaviors.

Thickening would involve the reverse inequality:

$$\nu_a(t\mathbf{v}) > \nu_a(\mathbf{v})$$

when $t > 1$. Often, the terminology suggests a particular flow regime such as shear, which we will study. But we will also consider a flow problem involving pure extension, in which $\nabla \mathbf{v}$ has quite different structure.

3. Oldroyd models

The simplest subset of the Oldroyd models involves three parameters, the fluid kinematic viscosity ν and two rheological parameters λ_1 and μ_1. This subset lacks any explicit dissipation mechanism, and Renardy (1985) suggested one way to incorporate one. Another approach was explored in Girault and Scott (2018) that has a strong theoretical base and provides an algorithm for approximation.

A three parameter subset of the eight parameter model of Oldroyd (1958) for the extra stress takes the form

$$\mathbf{T} + \lambda_1(\mathbf{u}\cdot\nabla\mathbf{T} + \mathbf{R}\circ\mathbf{T} + \mathbf{T}\circ\mathbf{R}^t) - \mu_1(\mathbf{E}\circ\mathbf{T} + \mathbf{T}\circ\mathbf{E}) = 2\nu\mathbf{E},$$

where the five parameters λ_2, μ_2, μ_0, ν_0, and ν_1 in Oldroyd (1958) are set to zero, and

$$\mathbf{R} = \tfrac{1}{2}(\nabla\mathbf{u}^t - \nabla\mathbf{u}) \text{ and } \mathbf{E} = \tfrac{1}{2}(\nabla\mathbf{u} + \nabla\mathbf{u}^t).$$

We have used the notation $\mathbf{T}\circ\mathbf{U}$ to mean tensor multiplication, which is in this case the same as matrix multiplication. Note that $\mathbf{E}^t = \mathbf{E}$, $\mathbf{R}^t = -\mathbf{R}$, $\mathbf{R} + \mathbf{E} = \nabla\mathbf{u}^t$, and $\mathbf{R} - \mathbf{E} = -\nabla\mathbf{u}$.

We can write the full model in the steady case as

$$\mathbf{u}\cdot\nabla\mathbf{u} + \nabla p = \nabla\cdot\mathbf{T} + \mathbf{f} \text{ in } \Omega, \quad \nabla\cdot\mathbf{u} = 0 \text{ in } \Omega, \quad \mathbf{u} = \mathbf{g} \text{ on } \partial\Omega, \tag{3.5}$$

$$\mathbf{T} + \lambda_1(\mathbf{u}\cdot\nabla\mathbf{T} + \mathbf{R}\circ\mathbf{T} + \mathbf{T}\circ\mathbf{R}^t) - \mu_1(\mathbf{E}\circ\mathbf{T} + \mathbf{T}\circ\mathbf{E}) = 2\nu\mathbf{E} \text{ in } \Omega. \tag{3.6}$$

The general case (3.6) can thus be written similarly as

$$\mathbf{T} + \lambda_1(\mathbf{u}\cdot\nabla\mathbf{T} - (\nabla\mathbf{u})\circ\mathbf{T} - \mathbf{T}\circ(\nabla\mathbf{u}^t)) + (\lambda_1 - \mu_1)(\mathbf{E}\circ\mathbf{T} + \mathbf{T}\circ\mathbf{E}) = 2\nu\mathbf{E}. \tag{3.7}$$

When $\lambda_1 = \mu_1 = \lambda$, (3.6) is known as the upper-convected Maxwellian model (Tanner 1982, Renardy 1985):

$$\mathbf{T} + \lambda_1(\mathbf{u}\cdot\nabla\mathbf{T} - (\nabla\mathbf{u})\circ\mathbf{T} - \mathbf{T}\circ(\nabla\mathbf{u}^t)) = 2\nu\mathbf{E}.$$

When $\lambda_1 = -\mu_1 = \lambda$, (3.6) is known as the lower-convected Maxwellian model. There are physical reasons to assume that $\lambda_1 > 0$, but we will allow $\lambda_1 < 0$ as well. The case $\lambda_1 = \mu_1 = 0$ corresponds to the incompressible Navier–Stokes equations.

The difficulty with this set of Oldroyd-type models is that there is no explicit dissipation (Girault and Scott 2018) in the basic equation (2.1).

3.1. Extensional flow

For a given constant speed U, extensional flow $\mathbf{u}(x,y) = U(x,-y)^t$, depicted in figure 1, exhibits a constraint for the Oldroyd models. This flow is evidently incompressible, and we will show that there is a corresponding solution with constant $\mathbf{T}$, so that $\nabla\cdot\mathbf{T} = 0$. We have

$$\mathbf{E} = \nabla\mathbf{u} = U\begin{pmatrix} 1 & 0 \\ 0 & -1 \end{pmatrix}, \qquad \mathbf{R} = 0. \tag{3.8}$$

Thus

$$\mathbf{u}\cdot\nabla\mathbf{u} = \mathbf{E}\mathbf{u} = U^2\begin{pmatrix} x \\ y \end{pmatrix} = \frac{U^2}{2}\nabla\left(x^2 + y^2\right),$$

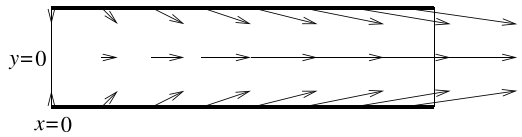

Figure 1. Extensional flow in a two-dimensional channel.

so we can take

$$p(x,y) = \frac{U^2}{2}\left(x^2+y^2\right) \tag{3.9}$$

and solve

$$-\beta\Delta\mathbf{u} + \mathbf{u}\cdot\nabla\mathbf{u} + \nabla p = 0 \text{ in } \Omega, \tag{3.10}$$

for any β.

3.2. *Extensional stress for 3 parameter Oldroyd*

If we take

$$\mathbf{u}(x,y) = U(x,-y)^t,$$

then (3.6) (for constant $\mathbf{T}$) simplifies to

$$\mathbf{T} - \mu_1(\mathbf{E}\circ\mathbf{T} + \mathbf{T}\circ\mathbf{E}) = 2\nu\mathbf{E}. \tag{3.11}$$

Suppose that

$$\mathbf{T} = \begin{pmatrix} a & b \\ b & c \end{pmatrix},$$

for unknown constants a, b, c. Then

$$\mathbf{E}\circ\mathbf{T} + \mathbf{T}\circ\mathbf{E} = U\begin{pmatrix} a & b \\ -b & -c \end{pmatrix} + U\begin{pmatrix} a & -b \\ b & -c \end{pmatrix} = 2U\begin{pmatrix} a & 0 \\ 0 & -c \end{pmatrix}.$$

From (3.8) and (3.11), we conclude that

$$\begin{pmatrix} a & b \\ b & c \end{pmatrix} - 2\mu_1 U\begin{pmatrix} a & 0 \\ 0 & -c \end{pmatrix} = 2\nu U\begin{pmatrix} 1 & 0 \\ 0 & -1 \end{pmatrix}.$$

Thus $b = 0$ and

$$a = \frac{2\nu U}{1-2\mu_1 U}, \qquad c = -\frac{2\nu U}{1+2\mu_1 U}. \tag{3.12}$$

We can simplify this using the expressions

$$\frac{1}{1-x} = 1 + \frac{x}{1-x}, \qquad \frac{1}{1+x} = 1 - \frac{x}{1+x}, \tag{3.13}$$

with $x = 2\mu_1 U$. Thus there is a solution with constant $\mathbf{T}$ given by

$$\begin{aligned} \mathbf{T} &= 2\nu U\begin{pmatrix} \frac{1}{1-2\mu_1 U} & 0 \\ 0 & -\frac{1}{1+2\mu_1 U} \end{pmatrix} \\ &= 2\nu U\begin{pmatrix} 1 & 0 \\ 0 & -1 \end{pmatrix} + 4\nu\mu_1 U^2\begin{pmatrix} \frac{1}{1-2\mu_1 U} & 0 \\ 0 & \frac{1}{1+2\mu_1 U} \end{pmatrix} \end{aligned} \tag{3.14}$$

for extensional flow $\mathbf{u}(x,y) = U(x,-y)^t$. The first part of the stress $\mathbf{T}$ is the Newtonian stress

$$\mathbf{T}_{\mathrm{N}} = 2\nu U \begin{pmatrix} 1 & 0 \\ 0 & -1 \end{pmatrix}$$

and the second part we can think of as the Oldroydian part:

$$\mathbf{T}_{\mathrm{O}} = 4\nu\mu_1 U^2 \begin{pmatrix} \frac{1}{1-2\mu_1 U} & 0 \\ 0 & \frac{1}{1+2\mu_1 U} \end{pmatrix}.$$

There is a well known singularity (Owens and Phillips 2002) for flow at speed

$$U = 1/2|\mu_1|. \tag{3.15}$$

For $\mu_1 > 0$, the coefficient a becomes singular for this value of U, and if μ_1 were negative, the coefficient c in (3.12) would be the one to indicate a singularity, instead of a. The limitation U on μ_1 can be viewed as a defect, but it can also be viewed as just a feature of the model. That is, it says that there is a limit on the size of $|\mu_1|$ related to the range of appropriate flow speeds being modeled.

By considering extensional flow for the Oldroyd model, we have learned that

- the parameter μ_1 can be very small and yet have a big effect, and
- the Oldroyd stress in extension does not depend directly on λ_1.

3.3. Extensional rheometer

We can imagine an extensional rheometer where we measure the normal stress on the outlet of the channel

$$\int_0^1 \mathbf{n}^t \mathbf{T}\mathbf{n}(L,y) - p(L,y)\,\mathrm{d}y, \tag{3.16}$$

where $\mathbf{n} = (1,0)^t$ and L indicates the end of the channel. Physically, we could put a membrane over the outlet and measure its deformation, at least for small deformations. The integral of the normal stress gives the force on the membrane.

If we are mainly interested in how (3.16) differs from Newtonian flow, this simplifies to be

$$\frac{4\nu U^2 \mu_1}{1-2\mu_1 U}, \tag{3.17}$$

since the pressure is the same for Newtonian flow. Thus the Oldroyd fluid can be shear-thickening or shear-thinning depending on the sign of μ_1.

3.4. Computing coefficients from data

The force F measured in the extensional flow rheometer, that is the Newtonian component together with the non-Newtonian force in (3.17), is

$$F(U) = 2\nu U + U^2 \left(\frac{4\nu\mu_1}{1-2\mu_1 U} - c_p \right), \tag{3.18}$$

where (3.9) implies that

$$c_p = U^{-2} \int_0^1 p(L,y)\,\mathrm{d}y = \int_0^1 (L^2 + y^2)\,\mathrm{d}y. \tag{3.19}$$

We claim that plotting (3.18) as a function of U allows identification of ν and μ_1, although it would give no information on λ_1. We will demonstrate this as follows.

We can measure the slope $s(U) = F'(U)$ from the plot of (3.18) as a function of U to get

$$s(U) = 2\nu + 4U\left(\frac{2\nu\mu_1}{1-2\mu_1 U} - c_p\right) + U^2\left(\frac{8\nu\mu_1^2}{(1-2\mu_1 U)^2}\right). \tag{3.20}$$

We have $2\nu = \lim_{U\to 0} s(U) = s(0)$. In particular, this shows that the extensional rheometer can measure the viscosity. Moreover,

$$\begin{aligned} s(U)/s(0) &= 1 + \frac{4\mu_1 U}{1-2\mu_1 U} - 4Uc_p/s(0) + \frac{(2\mu_1 U)^2}{(1-2\mu_1 U)^2} \\ &= 1 + 2f(2\mu_1 U) - 4Uc_p/s(0) + f(2\mu_1 U)^2, \end{aligned} \tag{3.21}$$

where

$$f(x) = x/(1-x). \tag{3.22}$$

Differentiating (3.21) with respect to U, we find

$$s'(U)/s(0) = -4c_p/s(0) + 4\mu_1 f'(2\mu_1 U)\big(1 + f(2\mu_1 U)\big).$$

Thus

$$s'(0)/s(0) = -4c_p/s(0) + 4\mu_1 f'(0) = -4c_p/s(0) + 4\mu_1, \tag{3.23}$$

so that $c_p/s(0) = \mu_1 - \frac{1}{4}s'(0)/s(0)$. Therefore

$$\begin{aligned} s(U)/s(0) &= 1 - 2U\big(\mu_1 - \tfrac{1}{4}s'(0)/s(0)\big) + 2f(2\mu_1 U) + f(2\mu_1 U)^2, \\ s'(U)/s(0) - s'(0)/s(0) &= 4\mu_1\Big(-1 + f'(x)\big(1+f(x)\big)\Big), x = 2\mu_1 U. \end{aligned} \tag{3.24}$$

But

$$\begin{aligned} g(x) &= f'(x)\big(1+f(x)\big) - 1 = \frac{1}{(1-x)^2}\frac{1}{1-x} - 1 \\ &= \frac{1}{(1-x)^3} - 1 = \frac{3x - 3x^2 + x^3}{(1-x)^3}. \end{aligned} \tag{3.25}$$

Thus

$$s'(U)/s(0) - s'(0)/s(0) = 4\mu_1 g(2\mu_1 U) = 4\mu_1 g(x), \quad x = 2\mu_1 U. \tag{3.26}$$

Moreover,

$$g'(x) = \big((1-x)^{-3} - 1\big)' = 3(1-x)^{-4} > 0, \quad 0 \leqslant x < 1, \tag{3.27}$$

so g is monotonically increasing. From (3.26)

$$\frac{U\big(s'(U) - s'(0)\big)}{s(0)} = 4\mu_1 U g(2\mu_1 U) = 2xg(x), \quad x = 2\mu_1 U. \tag{3.28}$$

Since g is monotonically increasing, the function ϕ defined by

$$\phi(x) = 2xg(x)$$

is also monotonically increasing for $0 \leqslant x < 1$. Thus we can write

$$\mu_1 = \frac{1}{2U}\phi^{-1}\left(\frac{U\big(s'(U) - s'(0)\big)}{s(0)}\right). \tag{3.29}$$

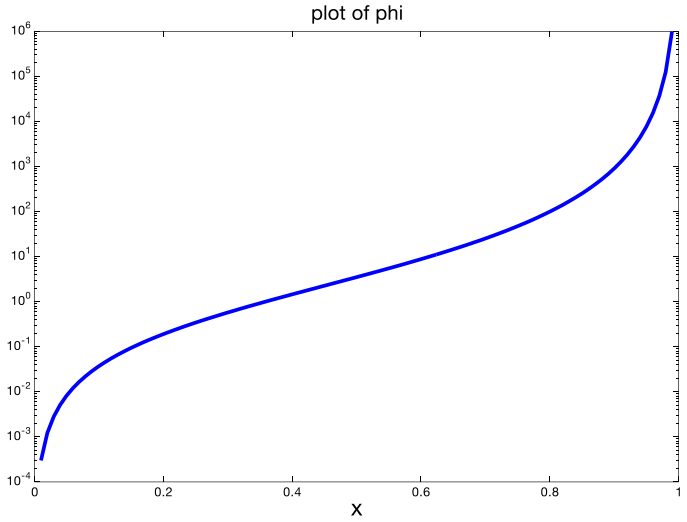

Figure 2. Plot of $xg(x) = \frac{1}{2}\phi(x)$ where g is defined in (3.25).

Note that solving $\phi(x) = d$ can easily be done via Newton's method. Both the slope and its derivative can be obtained reliably from the data via the Savitsky–Golay algorithm (Scott and Scott 1989). The value of μ_1 can thus be reliably estimated by averaging (3.29) over a suitable range of U values. A plot of $\frac{1}{2}\phi$ is in figure 2.

To get a more precise understanding of the behavior of μ_1 on the data, we can also write

$$xg(x) = x\frac{3x-3x^2+x^3}{(1-x)^3} = x^2q(x), \quad \text{where } q(x) = \frac{3-3x+x^2}{(1-x)^3}.$$

Then

$$\begin{aligned} q'(x) &= \frac{(-3+2x)(1-x)^3+3\big(3-3x+x^2\big)(1-x)^2}{(1-x)^6} \\ &= \frac{(-3+2x)(1-x)+3\big(3-3x+x^2\big)}{(1-x)^4} \\ &= \frac{(-3+5x-2x^2)+\big(9-9x+3x^2\big)}{(1-x)^4} \\ &= \frac{6-4x+x^2}{(1-x)^4} = \frac{2+(x-2)^2}{(1-x)^4} \geqslant 3(1-x)^{-4},\ 0 \leqslant x < 1. \end{aligned} \tag{3.30}$$

Therefore, q is strictly increasing for $0 \leqslant x < 1$. For U small, we have

$$f(x) = xg(x) = x^2q(x) = \frac{U\big(s'(U)-s'(0)\big)}{s(0)} \approx U^2\frac{s''(0)}{s(0)}, \tag{3.31}$$

so that

$$q(0)x^2 = 3x^2 \approx U^2\frac{s''(0)}{s(0)},$$

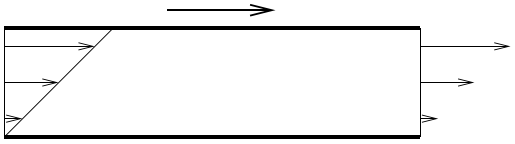

Figure 3. Shear flow in a two-dimensional channel. the upper channel wall is moving.

and hence

$$x \approx U\sqrt{\frac{s''(0)}{3s(0)}} \implies \mu_1 \approx \sqrt{\frac{s''(0)}{12s(0)}}. \tag{3.32}$$

We do not need to differentiate the slope of the data twice to compute μ_1 via the formula (3.29). Inverting the function ϕ can be done numerically to high accuracy via Newton's method, without relying on any smoothness of the data.

3.5. Shear flow

We consider two-dimensional flow in a channel $\Omega = [-L, L] \times [0, 1]$. Couette, or shear, flow, has $\mathbf{u} = U(y, 0)^t$ and p constant if $\mathbf{T}$ is constant as shown in figure 3. Now we consider (3.7). We have

$$\begin{aligned} \nabla\mathbf{u} &= \begin{pmatrix} 0 & U \\ 0 & 0 \end{pmatrix}, \quad \mathbf{E} = \frac{1}{2}\begin{pmatrix} 0 & U \\ U & 0 \end{pmatrix}, \quad \mathbf{R} = \frac{1}{2}\begin{pmatrix} 0 & -U \\ U & 0 \end{pmatrix}, \\ \mathbf{R}^t &= \frac{1}{2}\begin{pmatrix} 0 & U \\ -U & 0 \end{pmatrix}, \end{aligned} \tag{3.33}$$

and suppose that

$$\mathbf{T} = \begin{pmatrix} a & b \\ b & c \end{pmatrix}.$$

Then

$$\mathbf{E}\circ\mathbf{T} + \mathbf{T}\circ\mathbf{E} = \frac{U}{2}\begin{pmatrix} b & c \\ a & b \end{pmatrix} + \frac{U}{2}\begin{pmatrix} b & a \\ c & b \end{pmatrix} = U\begin{pmatrix} b & \frac{1}{2}(a+c) \\ \frac{1}{2}(a+c) & b \end{pmatrix}.$$

Similarly,

$$\mathbf{R}\circ\mathbf{T} + \mathbf{T}\circ\mathbf{R}^t = \frac{U}{2}\begin{pmatrix} -b & -c \\ a & b \end{pmatrix} + \frac{U}{2}\begin{pmatrix} -b & a \\ -c & b \end{pmatrix} = U\begin{pmatrix} -b & \frac{1}{2}(a-c) \\ \frac{1}{2}(a-c) & b \end{pmatrix}.$$

Therefore

$$\begin{aligned} &\mathbf{T} + \lambda_1\big(\mathbf{R}\circ\mathbf{T} + \mathbf{T}\circ\mathbf{R}^t\big) - \mu_1(\mathbf{E}\circ\mathbf{T} + \mathbf{T}\circ\mathbf{E}) \\ &\quad = \begin{pmatrix} a - U(\lambda_1+\mu_1)b & b + \frac{1}{2}U\big(\lambda_1(a-c) - \mu_1(a+c)\big) \\ b + \frac{1}{2}U\big(\lambda_1(a-c) - \mu_1(a+c)\big) & c + U(\lambda_1-\mu_1)b \end{pmatrix}. \end{aligned} \tag{3.34}$$

Therefore the equation

$$\mathbf{T} - \lambda_1\big((\nabla\mathbf{u})\circ\mathbf{T} + \mathbf{T}\circ(\nabla\mathbf{u})^t\big) = 2\nu\mathbf{E} = \nu\begin{pmatrix} 0 & U \\ U & 0 \end{pmatrix}$$

reduces to

$$a=(\lambda_1+\mu_1)bU,\quad c=-(\lambda_1-\mu_1)bU,\quad a-c=2\lambda_1 bU,\quad a+c=2\mu_1 bU,$$

so that

$$\begin{aligned}\nu U &= b+\tfrac{1}{2}\lambda_1(a-c)U-\tfrac{1}{2}\mu_1(a+c)U\\ &= b\big(1+(U)^2(\lambda_1^2-\mu_1^2)\big).\end{aligned}\tag{3.35}$$

Therefore

$$b=\frac{\nu U}{1+(U)^2(\lambda_1^2-\mu_1^2)}.$$

Thus

$$a=(\lambda_1+\mu_1)bU=\frac{\nu(\lambda_1+\mu_1)U^2}{1+U^2(\lambda_1^2-\mu_1^2)},\quad c=\frac{-\nu(\lambda_1-\mu_1)U^2}{1+U^2(\lambda_1^2-\mu_1^2)},$$

and so

$$\mathbf{T}=\frac{\nu}{1+U^2(\lambda_1^2-\mu_1^2)}\begin{pmatrix}(\lambda_1+\mu_1)U^2 & U\\ U & -(\lambda_1-\mu_1)U^2\end{pmatrix}.\tag{3.36}$$

Let us define the stress $\mathbf{T}_{\rm N}$ for Newtonian shear flow by

$$\mathbf{T}_{\rm N}=\nu U\begin{pmatrix}0 & 1\\ 1 & 0\end{pmatrix},\tag{3.37}$$

and we can denote the Oldroyd stress (3.36) by $\mathbf{T}_{\rm O}$. Then

$$\mathbf{T}_{\rm O}=\frac{1}{1+U^2(\lambda_1^2-\mu_1^2)}\mathbf{T}_{\rm N}+\frac{\nu U^2}{1+U^2(\lambda_1^2-\mu_1^2)}\begin{pmatrix}\lambda_1+\mu_1 & 0\\ 0 & -\lambda_1+\mu_1\end{pmatrix}.\tag{3.38}$$

3.6. Shear rheometer

We can imagine a rheometer based on shear flow, as follows. We have a rotating belt at the top of the channel enforcing the velocity $U(1,0)$. If we did not constrain the bottom of the channel, the whole apparatus would move to the right. So we measure the force required to keep it in place. This force must be balanced by the fluid shear stress

$$\int_{-L}^{L}\mathbf{n}^t\mathbf{T}_{\rm O}\mathbf{t}(x,0)\,{\rm d}x.\tag{3.39}$$

Here, $\mathbf{n}=(0,-1)$ is the outward normal to the bottom of the channel, and $\mathbf{t}=(1,0)$ is tangent to the bottom. But

$$\begin{pmatrix}\lambda_1+\mu_1 & 0\\ 0 & -\lambda_1+\mu_1\end{pmatrix}\begin{pmatrix}1\\0\end{pmatrix}=\begin{pmatrix}\lambda_1+\mu_1\\0\end{pmatrix}\tag{3.40}$$

so that

$$\mathbf{n}^t\begin{pmatrix}\lambda_1+\mu_1 & 0\\ 0 & -\lambda_1+\mu_1\end{pmatrix}\mathbf{t}=0.\tag{3.41}$$

Thus the force measured for an Oldroyd fluid is the same as that measured for a Newtonian fluid, multiplied by

$$\frac{1}{1+U^2(\lambda_1^2-\mu_1^2)}.$$

Plotting

$$f(U) = \frac{2\nu U}{1 + U^2(\lambda_1^2 - \mu_1^2)}$$

as a function of U would allow identification of both ν and $\lambda_1^2 - \mu_1^2$, but it would not determine λ_1 and μ_1 separately. But if we combine this with the results of the extensional rheometer, we can recover λ_1, although the sign would be ambiguous. In particular,

$$f(U) + U^2\lambda_1^2 f(U) = U^2\mu_1^2 f(U) + 2\nu U.$$

Thus

$$\lambda_1^2 = \frac{U^2\mu_1^2 f(U) + 2\nu U - f(U)}{U^2 f(U)} = \mu_1^2 + \frac{2\nu U - f(U)}{U^2 f(U)}.$$

Note that for small U,

$$f(U) \approx 2\nu U\Big(1 - U^2(\lambda_1^2 - \mu_1^2) + \big(U^2(\lambda_1^2 - \mu_1^2)\big)^2 + \mathcal{O}(U^6)\Big),$$

so that

$$\begin{aligned} \frac{2\nu U - f(U)}{U^2 f(U)} &\approx \frac{2\nu U^3(\lambda_1^2 - \mu_1^2) + 2\nu U^5(\lambda_1^2 - \mu_1^2)^2 + \mathcal{O}(U^7)}{2\nu U^3 + \mathcal{O}(U^5)} \\ &\approx \lambda_1^2 - \mu_1^2 + \frac{U^2(\lambda_1^2 - \mu_1^2)^2 + \mathcal{O}(U^4)}{1 + \mathcal{O}(U^2)} \end{aligned} \tag{3.42}$$

remains bounded as $U \to 0$.

3.7. Oldroyd rheometer conclusions

We have shown that a shear-flow rheometer can be used to determine both ν and the combination $\lambda_1^2 - \mu_1^2$, whereas the extensional-flow rheometer can be used to determine both ν and μ_1, but not λ_1. Combining measurements from these two rheometers allows the determination of all three coefficients, and it includes a cross check on the viscosity parameter ν.

4. Grade-two fluid model

The grade-two model of Ericksen and Rivlin (1997), Girault and Scott (1999) can be expressed as a single equation. The stress tensor for the grade-two fluid model satisfies

$$\mathbf{T} = \nu\mathbf{A} + \alpha_1 \frac{\Delta}{\Delta t}\mathbf{A} + \alpha_2 \mathbf{A}^2,$$

where $\mathbf{A} = (\nabla\mathbf{u}) + (\nabla\mathbf{u})^t = 2\mathbf{E}$ and the material derivative and the lower-convected Oldroydian derivative are given by

$$\frac{\mathrm{D}}{\mathrm{D}t}\mathbf{f} := \left(\frac{\partial}{\partial t} + \mathbf{u}\cdot\nabla\right)\mathbf{f}, \qquad \frac{\Delta}{\Delta t}\mathbf{f} := \frac{\mathrm{D}}{\mathrm{D}t}\mathbf{f} + \mathbf{f}(\nabla\mathbf{u}) + (\nabla\mathbf{u})^t\mathbf{f}, \tag{4.43}$$

for any tensor-valued function $\mathbf{f}$. For the steady-state, grade-two fluid model, the stress tensor simplifies to

$$\mathbf{T} = \nu\mathbf{A} + \alpha_1\big(\mathbf{u}\cdot\nabla\mathbf{A} + \mathbf{A}\circ(\nabla\mathbf{u}) + (\nabla\mathbf{u})^t\circ\mathbf{A}\big) + \alpha_2\mathbf{A}\circ\mathbf{A}, \tag{4.44}$$

where the operator $\circ$ is just matrix multiplication, but it has been made explicit to simplify interpretation. Thus the equations of steady fluid motion (2.1) can be written

$$-\nu\,\Delta\,\mathbf{u}+\mathbf{u}\cdot\nabla\mathbf{u}+\nabla p=\nabla\cdot\mathbf{T}_{\rm G},\quad \nabla\cdot\mathbf{u}=0\quad\text{in }\Omega,\quad \mathbf{u}=\mathbf{g}\quad\text{on }\partial\Omega. \tag{4.45}$$

Here

$$\begin{aligned}\mathbf{T}_{\rm G}&=\mathbf{T}-\nu\mathbf{A}=\alpha_1\big(\mathbf{u}\cdot\nabla\mathbf{A}+\mathbf{A}\circ(\nabla\mathbf{u})+(\nabla\mathbf{u})^t\circ\mathbf{A}\big)+\alpha_2\mathbf{A}\circ\mathbf{A}\\&=\alpha_1\big(\mathbf{u}\cdot\nabla\mathbf{A}-\mathbf{A}\circ(\nabla\mathbf{u})^t-(\nabla\mathbf{u})\circ\mathbf{A}\big)+(\alpha_1+\alpha_2)\mathbf{A}\circ\mathbf{A}.\end{aligned} \tag{4.46}$$

4.1. Extensional flow

We saw in section 3.2 that extensional flow, given by

$$\mathbf{u}(x,y)=U(x,-y)^t\quad\text{and}\quad p(x,y)=\frac{U^2}{2}\big(x^2+y^2\big),$$

is a solution of the Navier–Stokes equations (3.10) in the domain depicted in figure 1. Thus we also have a solution of the grade-two model in that domain provided that

$$\alpha_1\big(\mathbf{u}\cdot\nabla\mathbf{A}+\mathbf{A}\circ(\nabla\mathbf{u})+(\nabla\mathbf{u})^t\circ\mathbf{A}\big)+\alpha_2\mathbf{A}\circ\mathbf{A} \tag{4.47}$$

is constant. Since $\nabla\mathbf{u}$ is symmetric in this case, we have

$$\mathbf{A}=2\nabla\mathbf{u}=2U\begin{pmatrix}1&0\\0&-1\end{pmatrix},$$

and thus $\mathbf{u}\cdot\nabla\mathbf{A}=0$ and

$$2\mathbf{A}\nabla\mathbf{u}=2\big(\nabla\mathbf{u}^t\mathbf{A}^t\big)^t=2\nabla\mathbf{u}^t\mathbf{A}=\mathbf{A}^2=4U^2\begin{pmatrix}1&0\\0&1\end{pmatrix}=4U^2\mathcal{I},$$

where $\mathcal{I}$ is the identity matrix. Thus the expression in (4.47) is constant. Then

$$\begin{aligned}\mathbf{T}&=\nu\mathbf{A}+\alpha_1\big(\mathbf{A}\circ(\nabla\mathbf{u})+(\nabla\mathbf{u})^t\circ\mathbf{A}\big)+\alpha_2\mathbf{A}\circ\mathbf{A}\\&=2\nu U\begin{pmatrix}1&0\\0&-1\end{pmatrix}+4(\alpha_1+\alpha_2)U^2\begin{pmatrix}1&0\\0&1\end{pmatrix}.\end{aligned} \tag{4.48}$$

4.2. Extensional flow rheometer

The extensional flow rheometer would report a difference from Newtonian flow for the normal stress at the outlet given by

$$\mathbf{T}_{\rm G}=4(\alpha_1+\alpha_2)U^2.$$

Thus the grade-two fluid can be shear-thickening or shear-thinning depending on the sign of $\alpha_1+\alpha_2$.

The force measured will be a combination of ν and $\alpha_1+\alpha_2$, namely

$$2\nu U+U^2\big(4(\alpha_1+\alpha_2)-c_p\big),$$

where c_p is defined in (3.19). By plotting the measured force against U, it is possible to determine both ν and $\alpha_1+\alpha_2$.

4.3. Shear flow: grade two

We saw in section 3.5 that $\mathbf{u} = U(y,0)^t$ and p is constant if $\mathbf{T}$ is constant. We have

$$\nabla\mathbf{u} = \begin{pmatrix} 0 & U \\ 0 & 0 \end{pmatrix}, \ \mathbf{A} = \begin{pmatrix} 0 & U \\ U & 0 \end{pmatrix}, \ \mathbf{A}\circ\mathbf{A} = \begin{pmatrix} U^2 & 0 \\ 0 & U^2 \end{pmatrix},$$
$$\mathbf{A}\circ\nabla\mathbf{u} = \nabla\mathbf{u}^t\circ\mathbf{A} = \begin{pmatrix} 0 & 0 \\ 0 & U^2 \end{pmatrix}.$$

Thus (4.44) implies that

$$\mathbf{T} = \nu U \begin{pmatrix} 0 & 1 \\ 1 & 0 \end{pmatrix} + 2\alpha_1 U^2 \begin{pmatrix} 0 & 0 \\ 0 & 1 \end{pmatrix} + \alpha_2 U^2 \begin{pmatrix} 1 & 0 \\ 0 & 1 \end{pmatrix}. \tag{4.49}$$

Here we have $\mathbf{T} = \mathbf{T}_\mathrm{N} + \mathbf{T}_\mathrm{G}$ where

$$\mathbf{T}_\mathrm{N} = \nu U \begin{pmatrix} 0 & 1 \\ 1 & 0 \end{pmatrix}, \qquad \mathbf{T}_\mathrm{G} = 2\alpha_1 U^2 \begin{pmatrix} 0 & 0 \\ 0 & 1 \end{pmatrix} + \alpha_2 U^2 \begin{pmatrix} 1 & 0 \\ 0 & 1 \end{pmatrix}.$$

4.4. Shear flow rheometer

The shear-flow rheometer described in section 3.6 for the grade-two model will measure the same quantity as in (3.39) but with $\mathbf{T}_\mathrm{O}$ replaced by $\mathbf{T}_\mathrm{G} = \mathbf{T} - \mathbf{T}_\mathrm{N}$. And like the Oldroyd model, $\mathbf{n}\mathbf{T}_\mathrm{G}\mathbf{t} = 0$, so the simple shear rheometer will give the same result as for a Newtonian fluid, independent of the parameters α_i. Thus a pure shear-flow rheometer will report ν and a pure extensional flow rheometer will report a combination of ν and $\alpha_1 + \alpha_2$. Combining the two rheometers, we can determine $\alpha_1 + \alpha_2$, but it does not seem possible to determine α_1 and α_2 separately with these two geometries alone.

4.5. Grade-two rheometer conclusions

We have seen that the simple shear-flow rheometer described here does not distinguish the coefficients α_1 and α_2 in the grade-two model, despite the fact that the induced stress difference $\mathbf{T}_\mathrm{G}$ is quite complex in shear. If we take the definition (2.4) for apparent shear, then the grade-two model is shear thinning when α_2 is sufficiently negative, and otherwise it is shear thickening (assuming $\alpha_1 > 0$ in both cases).

5. Tanner duality

Tanner (1982) realized that there is a duality between the grade-two model (Girault and Scott 2001) and the Oldroyd models Girault and Scott (2018). This duality has been studied more recently from a mathematical perspective (Girault and Scott 2021a, 2021b). More precisely, Tanner observed that the solutions of grade-two were asymptotically the same as those for Oldroyd, with the parameters related by

$$\alpha_1 = -\nu\lambda_1, \qquad \alpha_1 + \alpha_2 = \nu\mu_1. \tag{5.50}$$

For clarity, let us write $\mathbf{T}^\mathrm{O}$ for the total Oldroyd stress, and $\mathbf{T}^\mathrm{G}$ for the total grade-two stress. We also write $\mathbf{T}_\mathrm{N}$ for the Newtonian stress. With the parameters related by (5.50), we expect that as $|\lambda_1| + |\mu_1| \to 0$,

$$\mathbf{T}^\mathrm{O} - \mathbf{T}^\mathrm{G} = \mathcal{O}(\lambda_1^2 + \mu_1^2) = \mathcal{O}(\alpha_1^2 + \alpha_2^2), \tag{5.51}$$

for fixed flow rate U and viscosity ν. Since we have computed stresses for these models in shear and extensional flow, we can compare them to test the range of validity of Tanner duality.

5.1. Extensional stresses

For extensional flow (section 3.1), the Newtonian stress $\mathbf{T}_{\rm N}$ and Oldroyd stress $\mathbf{T}^{\rm O}$ are given in (3.14):

$$\mathbf{T}_{\rm N} = 2\nu U \begin{pmatrix} 1 & 0 \\ 0 & -1 \end{pmatrix}, \qquad \mathbf{T}^{\rm O} = \mathbf{T}_{\rm N} + 4\nu\mu_1 U^2 \begin{pmatrix} \frac{1}{1-2\mu_1 U} & 0 \\ 0 & \frac{1}{1+2\mu_1 U} \end{pmatrix}. \tag{5.52}$$

Thus $\mathbf{T}^{\rm O} - \mathbf{T}_{\rm N} = \mathcal{O}(\mu_1)$. By contrast, the grade-two stress $\mathbf{T}^{\rm G}$ is given in (4.48) as

$$\mathbf{T}^{\rm G} = \mathbf{T}_{\rm N} + 4(\alpha_1+\alpha_2)U^2 \begin{pmatrix} 1 & 0 \\ 0 & 1 \end{pmatrix} = \mathbf{T}_{\rm N} + 4\nu\mu_1 U^2 \begin{pmatrix} 1 & 0 \\ 0 & 1 \end{pmatrix}, \tag{5.53}$$

where we have invoked (5.50). Thus we see that $\mathbf{T}^{\rm G} - \mathbf{T}_{\rm N} = \mathcal{O}(\mu_1)$. But more importantly, we can use (3.13) to show that

$$\begin{aligned} \mathbf{T}^{\rm O} - \mathbf{T}^{G} &= 4\nu\mu_1 U^2 \left(\begin{pmatrix} \frac{1}{1-2\mu_1 U} & 0 \\ 0 & \frac{1}{1+2\mu_1 U} \end{pmatrix} - \begin{pmatrix} 1 & 0 \\ 0 & 1 \end{pmatrix} \right) \\ &= 8\nu\mu_1^2 U^3 \begin{pmatrix} \frac{1}{1-2\mu_1 U} & 0 \\ 0 & \frac{-1}{1+2\mu_1 U} \end{pmatrix} = \mathcal{O}(\mu_1^2), \end{aligned} \tag{5.54}$$

in agreement with Tanner duality. On the other hand, $\mathbf{T}^{\rm O}$ and $\mathbf{T}^{\rm G}$ diverge rapidly as $U \to 1/2|\mu_1|$ in accordance with (3.15). Note that $\mathbf{T}^{\rm G}$ displays no singularity in this limit.

5.2. Shear stresses

For shear flow (section 3.5), the Newtonian stress $\mathbf{T}_{\rm N}$ and Oldroyd stress $\mathbf{T}^{O}$ are given in (3.38):

$$\begin{aligned} \mathbf{T}_{\rm N} &= \nu U \begin{pmatrix} 0 & 1 \\ 1 & 0 \end{pmatrix}, \\ \mathbf{T}^{O} &= \frac{1}{1+U^2(\lambda_1^2-\mu_1^2)}\mathbf{T}_{\rm N} + \frac{\nu U^2}{1+U^2(\lambda_1^2-\mu_1^2)} \begin{pmatrix} \lambda_1+\mu_1 & 0 \\ 0 & -\lambda_1+\mu_1 \end{pmatrix}. \end{aligned} \tag{5.55}$$

Therefore

$$\left(1+U^2(\lambda_1^2-\mu_1^2)\right)\mathbf{T}^{\rm O} = \mathbf{T}_{\rm N} + \nu U^2\lambda_1 \begin{pmatrix} 1 & 0 \\ 0 & -1 \end{pmatrix} + \nu U^2\mu_1 \begin{pmatrix} 1 & 0 \\ 0 & 1 \end{pmatrix}.$$

By contrast, the grade-two stress $\mathbf{T}^{\rm G}$ is given in (4.49) as

$$\begin{aligned} \mathbf{T}^{\rm G} &= \mathbf{T}_{\rm N} + 2\alpha_1 U^2 \begin{pmatrix} 0 & 0 \\ 0 & 1 \end{pmatrix} + \alpha_2 U^2 \begin{pmatrix} 1 & 0 \\ 0 & 1 \end{pmatrix} \\ &= \mathbf{T}_{\rm N} + U^2 \begin{pmatrix} \alpha_2 & 0 \\ 0 & 2\alpha_1+\alpha_2 \end{pmatrix} \\ &= \mathbf{T}_{\rm N} - \alpha_1 U^2 \begin{pmatrix} 1 & 0 \\ 0 & -1 \end{pmatrix} + (\alpha_1+\alpha_2)U^2 \begin{pmatrix} 1 & 0 \\ 0 & 1 \end{pmatrix}. \end{aligned} \tag{5.56}$$

Therefore invoking (5.50), we see that

$$\left(1+U^2(\lambda_1^2-\mu_1^2)\right)\mathbf{T}^{\rm O} = \mathbf{T}^{\rm G}. \tag{5.57}$$

Thus

$$\mathbf{T}^{\mathrm{O}} - \mathbf{T}^{\mathrm{G}} = U^2(\lambda_1^2 - \mu_1^2)\mathbf{T}^{\mathrm{O}}, \tag{5.58}$$

again confirming Tanner duality.

5.3. Model complementarity

Tanner duality allows us to pick models appropriately that match certain experiments. Let us re-examine shear flow and postulate a rheometer that measures the normal force on the top and bottom of the domain. Such a theoretical rheometer shares some features with the Lodge rheometer (Lodge *et al* 1991).

Let us simplify to the case where $\mu_1 = \alpha_1 + \alpha_2 = 0$. The Newtonian stress contributes nothing to the normal force, and the pressure is constant in shear flow, so the normal force is proportional to λ_1 for the Oldroyd model and $-\alpha_1$ for the grade-two model, where the constants of proportionality have the same sign. We can imagine two complementary materials A and B, one that pushes out on the channel walls and one that pulls in, as the fluids are sheared. Both types of materials are known in solid mechanics, so one cannot say *a priori* either is unrealistic. Then picking the Oldroyd model for material A might require $\lambda_1 < 0$, which has several drawbacks from a modeling perspective. Correspondingly, picking the grade-two model for material B would require $\alpha_1 < 0$, with its own set of drawbacks. However, picking the Oldroyd model for material B would have $\lambda_1 > 0$ due to Tanner duality, so it would be the preferred model for simulation. Similarly, picking the grade-two model for material A would have $\alpha_1 > 0$ due to Tanner duality, so it would be the preferred model for simulation.

6. Real rheometers

There is a variety of actual rheometers that are employed to make measurements. Here we describe just a few.

6.1. Contraction rheometers

A rheometer that emphasizes extensional flow is based on a contraction nozzle (Nyström *et al* 2017). Fluid is forced through the contraction either by pressure or a rod. The flow domain is defined by

$$\Omega = \left\{(x,y,z) \;\middle|\; b \leqslant z \leqslant t,\ x^2 + y^2 \leqslant f\left(x^2 + y^2\right)\right\}$$

for a given function f.

Since the two theoretical rheometers fail to detect α_1 for the grade-two fluid, a natural question is whether or not a contraction rheometer can do so. Since the extensional flow rheometer detects $\alpha_1 + \alpha_2$, a natural approach is the consider the special case $\alpha_1 + \alpha_2 = 0$, for which the grade-two model simplifies (Girault and Scott 1999, 2001). Similarly, it makes sense to consider a two-dimensional contraction as a first step, again simplifying the grade-two model. Such a geometry is considered in Pollock and Scott (2022b).

6.2. Counter-rotating cylinders

One common type of rheometer is based on counter-rotating concentric cylinders, essentially the original experiment of Couette (Gallot *et al* 2013). What is measured is the torque on one cylinder induced by the other cylinder. For example, the outer cylinder is rotated at a fixed

speed and the torque on the inner cylinder required to keep it stationary is recorded. This measures quantities similar to our pure shear rheometer, so we do not pursue this further here.

6.3. X-plate rheometers

There are two different, but related rheometers that involve a plate below and either (a) a cone above or (b) a parallel plate above. For example, the lower plate could be fixed and the upper structure rotated. Thus one obtains the cone-and-plate rheometer (Markovitz *et al* 1955, Ellenberger and Fortuin 1985) and the parallel-plate rheometer (Yamamoto 1958, Ellenberger and Fortuin 1985). In both cases, the geometry and (steady) flow have radial symmetry.

6.4. Hole-pressure difference rheometer

Lodge (1996) constructed a device to measure normal stress differences. The flow in a two-dimensional version of this device has been proposed as a test problem (Lodge *et al* 1991). Such approaches have been used effectively in rheological measurements in food technology (Padmanabhan and Bhattacharya 1993).

6.5. Journal bearing flow

In Robert *et al* (1985), two-dimensional computational simulations of journal bearings were used to evaluate six different rheological models.

7. Thick or thin

We summarize here the results of the exact solutions for both rheological models. Our objective is help assess whether models are thinning or thickening in different contexts. There are two issues to consider. First of all, does the stress change with changing flow rate or strain rate in a substantial way? If it does, does a particular rheometer report that change? We have noted the shortcoming of the shear rheometer for grade-two fluids. But we can see that it is not due to a lack of change of the stress itself.

Since the stress is a symmetric tensor, in two dimensions any stress can be written in terms of three basis vectors:

$$\mathcal{I} = \begin{pmatrix} 1 & 0 \\ 0 & 1 \end{pmatrix}, \qquad \mathcal{J} = \begin{pmatrix} 1 & 0 \\ 0 & -1 \end{pmatrix}, \qquad \mathcal{K} = \begin{pmatrix} 0 & 1 \\ 1 & 0 \end{pmatrix}. \tag{7.59}$$

In general, we can write

$$\begin{pmatrix} \alpha & \beta \\ \beta & \gamma \end{pmatrix} = \tfrac{1}{2}(\alpha+\gamma)\mathcal{I} + \tfrac{1}{2}(\alpha-\gamma)\mathcal{J} + \beta\mathcal{K}. \tag{7.60}$$

Suppose we choose the norm in (2.4) to be the Frobenius norm

$$\|(a_{ij})\|_F = \sqrt{\sum_{ij} a_{ij}^2}\,.$$

This is the norm associated with the inner-product

$$\big((a_{ij}),(b_{ij})\big)_F = \sum_{ij} a_{ij} b_{ij}.$$

In this inner-product, $\mathcal{I}$, $\mathcal{J}$, and $\mathcal{K}$ are all orthogonal and have Frobenius norm equal to $\sqrt{2}$. Thus

$$\|\, a\mathcal{I} + b\mathcal{J} + c\mathcal{K} \,\|_F = \sqrt{2\big(a^2+b^2+c^2\big)}. \tag{7.61}$$

Now let us use the representation (7.60) to describe our previous calculations of stresses in different flow regimes.

7.1. Oldroyd extensional flow

We first need to resolve the matrix on the right in (3.14). Using (7.60), we have

$$\begin{aligned}\begin{pmatrix} \frac{1}{1-2\mu_1 U} & 0 \\ 0 & \frac{1}{1+2\mu_1 U} \end{pmatrix} &= \frac{1}{2}\left(\frac{1}{1-2\mu_1 U} + \frac{1}{1+2\mu_1 U}\right)\mathcal{I} \\ &\quad + \frac{1}{2}\left(\frac{1}{1-2\mu_1 U} - \frac{1}{1+2\mu_1 U}\right)\mathcal{J} \\ &= \frac{1}{1-(2\mu_1 U)^2}\big(\mathcal{I} + 2\mu_1 U\mathcal{J}\big).\end{aligned} \tag{7.62}$$

Therefore

$$\mathbf{T}_{\rm N} = 2\nu U\mathcal{J}, \qquad \mathbf{T} = \mathbf{T}_{\rm N} + \frac{4\nu\mu_1 U^2}{1-(2\mu_1 U)^2}\big(\mathcal{I} + 2\mu_1 U\mathcal{J}\big).$$

Thus

$$\begin{aligned}\|\,\mathbf{T}\,\|_F^2 &= \left(2\nu U + \frac{8\nu\mu_1^2 U^3}{1-(2\mu_1 U)^2}\right)^2 + \left(\frac{4\nu\mu_1 U^2}{1-(2\mu_1 U)^2}\right)^2 \\ &= (2\nu U)^2\left(1 + \frac{4\mu_1^2 U^2}{1-(2\mu_1 U)^2}\right)^2 + (2\nu U)^2\left(\frac{2\mu_1 U}{1-(2\mu_1 U)^2}\right)^2 \\ &= (2\nu U)^2\left(\frac{1}{1-(2\mu_1 U)^2}\right)^2 + (2\nu U)^2\left(\frac{2\mu_1 U}{1-(2\mu_1 U)^2}\right)^2 \\ &= \frac{(2\nu U)^2}{\big(1-(2\mu_1 U)^2\big)^2}\big(1+(2\mu_1 U)^2\big).\end{aligned} \tag{7.63}$$

The strain (3.8) for extensional flow is proportional to U, so the apparent viscosity (2.4) tends to infinity as $U \to 1/2|\mu_1|$, and this would be described as extensional thickening.

7.2. Oldroyd shear flow

From (3.38), we find

$$\mathbf{T}_{\rm N} = \nu U\mathcal{K}, \quad \mathbf{T} = \frac{1}{1+U^2(\lambda_1^2-\mu_1^2)}\Big(\mathbf{T}_{\rm N} + \nu U^2\big(\lambda_1\mathcal{J} + \mu_1\mathcal{I}\big)\Big).$$

If $\lambda_1 = \mu_1$, this simplifies to

$$\mathbf{T} = \mathbf{T}_{\rm N} + \nu U^2\lambda_1\big(\mathcal{J}+\mathcal{I}\big).$$

In this special case,

$$\|\,\mathbf{T}\,\|_F^2 = (\nu U)^2\big(1+2U^2\lambda_1^2\big),$$

and asymptotically as $U \to \infty$,

$$\|\mathbf{T}\|_F \approx \nu U(1+\sqrt{2}U\lambda_1).$$

In the general case,

$$\|\mathbf{T}\|_F^2 = (\nu U)^2 \frac{1+U^2\left(\lambda_1^2+\mu_1^2\right)}{\left(1+U^2(\lambda_1^2-\mu_1^2)\right)^2} = \nu^2 \frac{U^{-2}+\left(\lambda_1^2+\mu_1^2\right)}{\left(U^{-2}+(\lambda_1^2-\mu_1^2)\right)^2}.$$

If $\lambda_1 \neq \pm\mu_1$, then

$$\|\mathbf{T}\|_F \to \nu \frac{\sqrt{\lambda_1^2+\mu_1^2}}{|\lambda_1^2-\mu_1^2|}.$$

as $U \to \infty$. This would qualify as shear thinning, since (3.33) implies that the Frobenius norm of the strain is proportional to U.

7.3. Grade-two extensional flow

From (4.48), we find

$$\mathbf{T}_{\mathrm{N}} = 2\nu U\mathcal{J}, \qquad \mathbf{T} = \mathbf{T}_{\mathrm{N}} + 4(\alpha_1+\alpha_2)U^2\mathcal{I}.$$

Thus

$$\|\mathbf{T}\|_F^2 = (2\nu U)^2 + 16(\alpha_1+\alpha_2)^2U^4.$$

Since the strain (3.8) for extensional flow is proportional to U, the apparent viscosity (2.4) grows monotonically as U increases, and this would be described as extensional thickening.

7.4. Grade-two shear flow

From (4.49), we find

$$\mathbf{T}_{\mathrm{N}} = \nu U\mathcal{K}, \quad \mathbf{T} = \mathbf{T}_{\mathrm{N}} + U^2\left(\alpha_1(\mathcal{I}-\mathcal{J})+\alpha_2\mathcal{I}\right) = \mathbf{T}_{\mathrm{N}} + U^2\left((\alpha_1+\alpha_2)\mathcal{I}-\alpha_1\mathcal{J}\right).$$

Thus

$$\|\mathbf{T}\|_F^2 = (\nu U)^2 + (\alpha_1+\alpha_2)^2U^4 + \alpha_1^2U^4.$$

Again, the strain (3.8) for shear flow is proportional to U, so the apparent viscosity (2.4) grows monotonically as U increases, and this would be described as shear thickening.

7.5. Other metrics

A norm is blunt instrument, but we saw in section 7.2 that it can identify shear thinning. But there may be a finer tool to analyze the impact of stress. The expression $\boldsymbol{\sigma}\mathbf{n}$ is the force on the plane perpendicular to the unit vector $\mathbf{n}$ due to the stress $\boldsymbol{\sigma}$. Then $\mathbf{n}^t\boldsymbol{\sigma}\mathbf{n}$ is the force due to $\boldsymbol{\sigma}$ in the direction $\mathbf{n}$, that is, against the surface represented by the plane. It $\mathbf{t}$ is another direction, then $\mathbf{t}^t\boldsymbol{\sigma}\mathbf{n}$ is the force due to $\boldsymbol{\sigma}$ in the direction $\mathbf{t}$. One direction of interest would be a direction tangent to the plane.

In the two-dimensional case, we can use the decomposition (7.60) for stresses and take $\mathbf{t}$ to be orthogonal to $\mathbf{n}$ and consider the force magnitudes

$$\mathbf{n}^t\boldsymbol{\sigma}\mathbf{n}, \qquad \mathbf{t}^t\boldsymbol{\sigma}\mathbf{n}.$$

These represent the 'observables' for $\boldsymbol{\sigma}$. Note that for symmetric $\boldsymbol{\sigma}$, $\mathbf{t}^t\boldsymbol{\sigma}\mathbf{n} = \mathbf{n}^t\boldsymbol{\sigma}\mathbf{t}$.

To quantify this, let us assume that

$$\mathbf{n} = (\cos\theta, \sin\theta), \qquad \mathbf{t} = (-\sin\theta, \cos\theta).$$

Then we have

$$\begin{aligned}
&\mathbf{n}^t\mathcal{I}\mathbf{n} = 1, \qquad \mathbf{t}^t\mathcal{I}\mathbf{n} = 0,\\
&\mathbf{n}^t\mathcal{J}\mathbf{n} = \cos^2\theta - \sin^2\theta = \cos 2\theta, \qquad \mathbf{t}^t\mathcal{J}\mathbf{n} = -2\cos\theta\sin\theta = -\sin 2\theta.\\
&\mathbf{n}^t\mathcal{K}\mathbf{n} = 2\cos\theta\sin\theta = \sin 2\theta, \qquad \mathbf{t}^t\mathcal{K}\mathbf{n} = \cos^2\theta - \sin^2\theta = \cos 2\theta.
\end{aligned}$$

Therefore

$$\begin{pmatrix} \mathbf{n}^t(a\mathcal{I} + b\mathcal{J} + c\mathcal{K})\mathbf{n} \\ \mathbf{t}^t(a\mathcal{I} + b\mathcal{J} + c\mathcal{K})\mathbf{n} \end{pmatrix} = \begin{pmatrix} a \\ 0 \end{pmatrix} + \begin{pmatrix} \cos 2\theta & \sin 2\theta \\ -\sin 2\theta & \cos 2\theta \end{pmatrix} \begin{pmatrix} b \\ c \end{pmatrix}. \tag{7.64}$$

We recognize the matrix in (7.64) as a rotation by -2θ.

As a first application, let us apply this methodology to Newtonian fluids. For shear flow, $\mathbf{T}_{\rm N} = \nu U\mathcal{K}$, and for extensional flow, $\mathbf{T}_{\rm N} = 2\nu U\mathcal{J}$. Thus

$$\begin{aligned}
\begin{pmatrix} \mathbf{n}^t\mathbf{T}_{\rm N}\mathbf{n} \\ \mathbf{t}^t\mathbf{T}_{\rm N}\mathbf{n} \end{pmatrix} &= \begin{pmatrix} \cos 2\theta & \sin 2\theta \\ -\sin 2\theta & \cos 2\theta \end{pmatrix} \begin{pmatrix} 2\nu U \\ 0 \end{pmatrix} \quad \text{(extensional flow)}\\
\begin{pmatrix} \mathbf{n}^t\mathbf{T}_{\rm N}\mathbf{n} \\ \mathbf{t}^t\mathbf{T}_{\rm N}\mathbf{n} \end{pmatrix} &= \begin{pmatrix} \cos 2\theta & \sin 2\theta \\ -\sin 2\theta & \cos 2\theta \end{pmatrix} \begin{pmatrix} 0 \\ \nu U \end{pmatrix} \quad \text{(shear flow).}
\end{aligned} \tag{7.65}$$

For example, if we take $\theta = 0$ (meaning the plane is perpendicular to the x-axis), then the normal force on this plane would be proportional to $2\nu U$ in extensional flow (with the shear stress zero), whereas the tangential force on this plane would be proportional to νU in shear flow (with the normal stress zero).

As another application, we apply this methodology to grade-two shear flow. Then

$$\begin{pmatrix} \mathbf{n}^t\mathbf{T}\mathbf{n} \\ \mathbf{t}^t\mathbf{T}\mathbf{n} \end{pmatrix} = \begin{pmatrix} U^2(\alpha_1 + \alpha_2) \\ 0 \end{pmatrix} + \begin{pmatrix} \cos 2\theta & \sin 2\theta \\ -\sin 2\theta & \cos 2\theta \end{pmatrix} \begin{pmatrix} -U^2\alpha_1 \\ \nu U \end{pmatrix}. \tag{7.66}$$

For $\theta = 0$, the normal force on the plane perpendicular to the x-axis is proportional to $U^2\alpha_2$. This could be measured with a net held initially in this plane, the deformation of the net being proportional to the force. Together with the measurement of $\alpha_1 + \alpha_2$ via the extensional flow rheometer, α_1 can then be determined.

8. Conclusions

We have studied the grade-two and Oldroyd 3-parameter models, and we computed solutions relevant to two hypothetical rheometers to see if the coefficients of the rheology models are identifiable from experimental measurements or not. For the Oldroyd models, we showed that the coefficients can be estimated from experiments from the two rheometers. But for the grade-two model, it was not possible to distinguish the two nonNewtonian parameters, only their sum can be estimated.

Acknowledgments

We would like to thank Sara Pollock and Tabea Tscherpel for valuable discussions. We also thank the referee for valuable suggestions.

ORCID iD

L Ridgway Scott https://orcid.org/0000-0002-7885-7106

References

Armstrong R C, Brown R A, Beris A N, Lawler J V and Muller S J 1985 Evaluation of constitutive equations: material functions and complex flows of viscoelastic fluids *Viscoelasticity and Rheology* ed J A Nohel, A S Lodge and M Renardy (Amsterdam: Elsevier) pp 361–89

Bird R B, Armstrong R C and Hassager O 1987 *Dynamics of Polymeric Liquids. Vol. 1: Fluid Mechanics* (New York: Wiley)

Cioranescu D, Girault V and Rajagopal K R 2016 *Mechanics and Mathematics of Fluids of the Differential Type* (Berlin: Springer)

Ellenberger J and Fortuin J M H 1985 A criterion for purely tangential laminar flow in the cone-and-plate rheometer and the parallel-plate rheometer *Chem. Eng. Sci.* **40** 111–6

Gallot T, Perge C, Grenard V, Fardin M-A, Taberlet N and Manneville Sebastien 2013 Ultrafast ultrasonic imaging coupled to rheometry: principle and illustration *Rev. Sci. Instrum.* **84** 045107

Girault V and Scott L R 1999 Analysis of a two-dimensional grade-two fluid model with a tangential boundary condition *J. Math. Pures Appl.* **78** 981–1011

Girault V and Scott L R 2001 Finite element discretizations of a two-dimensional grade-two fluid model *MMAN* **35** 1007–53

Girault V and Scott L R 2018 Oldroyd models without explicit dissipation *Rev. Roumaine Math. Pures Appl.* **63** 401–46

Girault V and Scott L R 2021a An asymptotic duality between the Oldroyd–Maxwell and grade-two fluid models. Research Report UC/CS TR-2021-08 Dept. Comp. Sci., Univ. Chicago

Girault V and Scott L R 2021b Tanner duality between the Oldroyd-Maxwell and grade-two fluid models *Comptes Rendus - Mathematiques* **359** 1207–15

Gokdogan O, Eryilmaz T and Yesilyurt M K 2015 Thermophysical properties of castor oil (Ricinus communis l.) Biodiesel and its blends *CT & F-Ciencia, Tecnología y Futuro* **6** 95–128

Joseph D D 2013 *Fluid Dynamics of Viscoelastic Liquids* vol 84 (New York: Springer Science & Business Media)

Kestin J, Sokolov M and Wakeham W A 1978 Viscosity of liquid water in the range - 8 c to 150 c *J. Phys. Chem. Ref. Data* **7** 941–8

Landau L D and Lifshitz E M 1959 *Fluid Mechanics* (Oxford: Pergamon)

Lodge A S 1996 On-line measurement of elasticity and viscosity in flowing polymeric liquids *Rheol. Acta* **35** 110–6

Lodge A S, Pritchard W G and Scott L R 1991 The hole–pressure problem *IMA J. Applied Math.* **46** 39–66

Markovitz H, Elyash L J, Padden Jr. F J and DeWitt T W 1955 A cone-and-plate viscometer *J. Colloid Sci.* **10** 165–73

Nijenhuis K, McKinley G, Spiegelberg S, Barnes H, Aksel N and Heymann L 2007 Non-newtonian flows *Springer Handbook of Experimental Fluid Mechanics* (Berlin: Springer) pp 619–743

Nunan K C and Keller J B 1984 Effective viscosity of a periodic suspension *J. Fluid Mech.* **142** 269–87

Nyström M, Jahromi H R T, Stading M and Webster M F 2017 Hyperbolic contraction measuring systems for extensional flow *Mech. Time-Depend. Mater.* **21** 455–79

Oldroyd J G 1958 Non-Newtonian effects in steady motion of some idealized elastico-viscous fluids *Proc. R. Soc.* A **245** 278–97

Owens R G and Phillips T N 2002 *Computational Rheology* (London: Imperial College Press)

Padmanabhan M and Bhattacharya M 1993 Effect of extrusion processing history on the rheology of corn meal *J. Food Eng.* **18** 335–49

Petrie C J S 2006 Extensional viscosity: a critical discussion *J. Non-Newton. Fluid Mech.* **137** 15–23

Pollock S and Scott L R 2022a An algorithm for the grade-two rheological model *M2AN* **56** 1007–25

Pollock S and Scott L R 2022b A contraction rheometer for identifying parameters in the grade-two fluid model *TBD*

Pollock S and Scott L R 2022c Transport equations with inflow boundary conditions *Partial Differ. Equ. Appl.* **3**

Renardy M 1985 Existence of slow steady flows of viscoelastic fluids with differential constitutive equations *Z. Angew. Math. Mech.* **65** 449–51
Rivlin R S and Ericksen J L 1997 Stress-deformation relations for isotropic materials *Collected Papers of RS Rivlin* (New York: Springer) pp 911–1013
Saramito P 2016 *Complex Fluids: Modeling and Algorithms* (Berlin: Springer)
Scott L B and Scott L R 1989 An efficient method for data smoothing via least–squares polynomial fitting *SIAM J. Num. Anal.* **26** 681–92
Tanner R I 1982 The stability of some numerical schemes for model viscoelastic fluids *J. Non-Newton. Fluid Mech.* **10** 169–74
Tanveer S, Sharma U C and Prasad R 2006 Rheology of multigrade engine oils *Indian J. Chem. Technol.* **13** 180–4
Yamamoto M 1958 The visco-elastic properties of network structure III. Normal stress effect (Weissenberg effect) *J. Phys. Soc. Japan* **13** 1200–11